*Desalination and Water Treatment*
www.deswater.com
doi: 10.1080/19443994.2013.794115

52 (2014) 2668–2677
March

Taylor & Francis
Taylor & Francis Group

# Photocatalytic degradation of chloramphenicol and tartrazine using Ag/TiO$_2$ nanoparticles

Akbar Jodat*, Asghar Jodat

*Laboratory of Chemistry, Shahindezh Branch, Islamic Azad University, Shahindezh, Iran*
*Tel. +98 4824221022; Fax: +98 4824229092; email: akbarjodat@gmail.com*

Received 9 January 2013; Accepted 30 March 2013

ABSTRACT

Photocatalytic degradation of chloramphenicol (CAP) and tartrazine (TAZ) was studied in the aqueous suspensions of silver-modified TiO$_2$ (Ag/TiO$_2$) nanoparticles under ultraviolet (UV) light irradiation. Ag/TiO$_2$ nanoparticles were prepared with chemical reduction method and characterized by X-ray diffraction (XRD), scanning electron micrographs (SEM), energy dispersive X-ray micro analysis (EDX), transmission electron microscope (TEM), and X-ray photoelectron spectroscopy (XPS) techniques. XPS measurement indicates that Ag mainly exists in the Ag$^0$ state on the TiO$_2$ nanoparticles surface. The effects of the operational parameters, such as silver concentration, photocatalyst loading, initial substrate concentration, light intensity, and calcination temperature were evaluated. It was found that the photocatalytic efficiency of TiO$_2$ nanoparticles for the degradation of CAP and TAZ can be significantly improved by depositing an optimum amount of Ag nanoparticles. By comparing the removal efficiency of CAP and TAZ at the similar conditions, it was observed that the photodegradation rate of TAZ was faster than that of CAP. Total organic carbon (TOC) removal was measured at optimum conditions to quantify the mineralization of the pollutants. Above 84 and 89% mineralization of CAP and TAZ was observed using 120 min irradiation.

*Keywords:* Photocatalytic degradation; Chloramphenicol; Tartrazine; Ag–TiO$_2$ nanoparticles; Chemical reduction

## 1. Introduction

Environmental pollution is the area of concern which inevitably requires deeper attention. Currently, due to industrial growth, the environmental pollution has been steadily escalated reaching to a critical level in the developing countries. In this regard, the discharge of effluents containing high concentrations of dyes and pharmacy wastewater pollutants has exacerbated the problem of environmental pollution. Dyes as water pollutants are nonbiodegradable and releasing them into the environment poses a significant threat to the surrounding ecosystems. Tartrazine (TAZ), one of them, although used as a cosmetic, drug, and food coloring dye, is considered highly toxic for humans due to its high solubility which is found in high amounts in industrial effluents [1–4].

Recently, a lot of studies have concentrated on the degradation of pharmacy wastewater pollutants. Pharmaceuticals including antibiotics are present in

---

*Corresponding author.

municipal sewage, largely as a result of human excretion. Antibiotic substances are not readily biodegradable and either pass through biological treatment plants intact or adsorb into the active sludge with subsequent desorption accumulating in the environment ultimately. It is clear that the presence of antibiotics in wastewaters and their abatement will be a significant challenge in the near future [5–7]. Among the antibiotics, chloramphenicol (CAP) is a broad-spectrum antibiotic exhibiting activity against both Gram-positive and Gram-negative bacteria, as well as other groups of micro-organisms. However, CAP is, in certain susceptible individuals, associated with serious toxic effects in humans including bone marrow depression, particularly severe in the form of fatal aplastic anemia [8–10].

In recent years, lots of efforts were made towards the development of new technologies for the degradation of water pollutions. In this field, the advanced oxidation processes (AOPs) is one of the major pathways for the near ambient degradation of wastewater contaminants, as they can provide almost total degradation. Although few studies on the performance of AOPs for oxidizing antibiotics are available, AOPs appear to be effective for oxidizing antimicrobial contaminants [11,12]. Among the various AOPs, heterogeneous semiconductor photocatalysis using $TiO_2$ as the photocatalyst is found capable of achieving complete oxidation of the water pollutants via the hydroxyl radicals ($^{\bullet}OH$) and/or valence band (vb) holes ($h^+$) generated when the semiconductor is exposed to UV irradiation [13–15]. The high rate of recombination between photogenerated electron–hole pairs is a major rate-determining factor controlling the photocatalytic efficiency. This efficiency can be improved by depositing noble metals on it. The presence of metal atoms or clusters may help the electron–hole separation by trapping photoelectrons and thereby facilitating the photo-oxidation. Among the various metals, namely Pt, Pd, Ag, Au, Rh, etc. that have been utilized for increasing the photocatalytic activity of semiconductors, silver (Ag) is particularly suitable for industrial applications due to its low cost and availability [16–18].

The different methods such as photodeposition, impregnation and other methods have been applied to prepare $Ag/TiO_2$ nanoparticles [19–21]. Nevertheless, there are rare studies concerning the photocatalytic degradation of pollutants using $Ag/TiO_2$ nanoparticles prepared by chemical reduction method [22]. Various researchers have studied the photodegradation of CAP and TAZ using pure $TiO_2$ nanoparticles [9,10,23]. In addition, there are many reports about the photocatalytic removal of similar pollutants [11,24–27]. To our knowledge, there is no systematic study dealing with comparative photocatalytic removal of an antibiotic and an azo dye with different molecular structure using $Ag/TiO_2$ nanoparticles obtained via chemical reduction methods.

In our recent study, the photocatalytic degradation of CAP and TAZ using pure $TiO_2$ and silver-modified $TiO_2$ nanoparticles in the presence of UV-irradiation has been investigated. $Ag/TiO_2$ nanoparticles have been synthesized by chemical reduction method and characterized using X-ray diffraction (XRD), scanning electron micrographs (SEM), X-ray micro analysis (EDX), transmission electron microscope (TEM), and X-ray photoelectron spectroscopy (XPS) techniques. Along the way, the effects of various operational parameters (silver concentration, photocatalyst loading, initial substrate concentration, light intensity, and calcination temperature) have been evaluated to maximize the degradation of CAP and TAZ under investigation. Extent of photodegradation and mineralization has been measured by using UV–vis spectrometer and total organic carbon (TOC) analyzer, respectively.

## 2. Experimental

### 2.1. Materials

CAP as a model antibiotic pollutant, and TAZ as a model pollutant from textile industry are purchased from Panreac and ACROS organics, respectively. Structure and other characteristics of the two pollutants are given in Table 1. $TiO_2$-P25 Degussa, 80% anatase, 20% rutile; BET area 50 $m^2/g$; primary size 21 nm were used as supporting material. Silver nitrate ($AgNO_3$, 99.9%) and sodium borohydride ($NaBH_4$, 98%) were purchased from Merck.

### 2.2. The preparation of $Ag/TiO_2$ nanoparticles

The $Ag/TiO_2$ nanoparticles were prepared by chemical reduction method. In this method, silver-modified $TiO_2$ nanoparticles were prepared by reducing $Ag^+$ ions to Ag metal on the $TiO_2$ surface. In this paper, $AgNO_3$ and $NaBH_4$ were used as source of silver ion and reducing agent, respectively. In brief, 2 g of $TiO_2$ was added to 100 mL of deionized water. Then the required amount of $AgNO_3$ was added into the suspension of $TiO_2$. Afterwards, a proper volume of $NaBH_4$ was added dropwise to the reaction mixture to obtain the Ag loadings of 0.25, 0.5, 1.0, 1.5, 2.0, and 2.5 wt.% in relation to $TiO_2$. The mixture was kept stirring vigorously by magnetic stirrer for 30 min. Finally, the suspensions were dried in an air oven at 100°C

Table 1
Structure and characteristics of CAP and TAZ

| | | |
|---|---|---|
| Chemical structure | 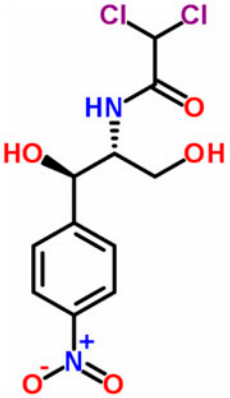 | 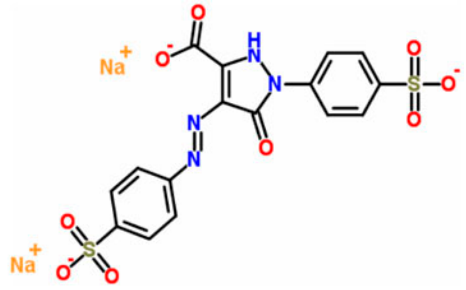 |
| Molecular formula | $C_{11}H_{12}Cl_2N_2O_5$ | $C_{16}H_9N_4Na_3O_9S_2$ |
| Other names | Alficetyn, amphicol, biomicin, chlornitromycin, chloromycetin, fenicol, phenicol, medicom, nevimycin, vernacetin, veticol | C.I. acid yellow 23, C.I. food yellow 4, E102, FD&C yellow 5 |
| IUPAC name | 2,2-Dichloro-*N*-[(1*R*,2*R*)-2-hydroxy-1-(hydroxymethyl)-2-(4-nitrophenyl)ethyl] acetamide | 4,5-Dihydro-5-oxo-1-(4-sulfophenyl)-4-[(4-sulfophenyl)azo]-1H-pyrazole-3-carboxylic acid trisodium |
| C.I. number | 56–75–7 | 19,140 |
| $\lambda_{max}$ (nm) | 275 | 429 |
| $M_w$ (g/mol) | 323.13 | 534.385 |

for 12 h and the dried solids were calcined at 300°C for 3 h in a furnace. The scheme of the preparation has been shown in Fig. 1.

### 2.3. Photoreactor and procedure

For the photocatalytic degradation of CAP and TAZ, a solution containing known concentration of pollutant (CAP or TAZ) and nanoparticle (pure or silver-modified $TiO_2$ nanoparticles) was allowed to equilibrate for 30 min in the darkness and then 100 mL of the prepared suspension was transferred into a borosilicate petri dish (12 cm diameter and 2.5 cm height) as a photoreactor. The reaction mixture was stirred vigorously under the illumination of UV-C light from top of the solution using a UV lamp (15 W, UV-C, $\lambda_{max} = 254$ nm manufactured by Philips, Holland). The distance of lamp from the solution was adjusted in such a way that light intensity of 50 W/m$^2$ was obtained on the surface of solution, which was measured by a Lux-UV-IR meter from Leybold Company. For kinetic studies, at certain reaction intervals, 5 mL of sample was withdrawn. To remove the Ag/$TiO_2$ particles from the reaction media, the solution was centrifuged for 15 min at 5,000 rpm. The concentration of CAP and TAZ was determined with a UV–vis spectrophotometer at 275 and 429 nm, respectively. Calibration plot based on Beer–Lambert's law was established by relating the absorbance to the concentration. All the photodegradation experiments were carried out at

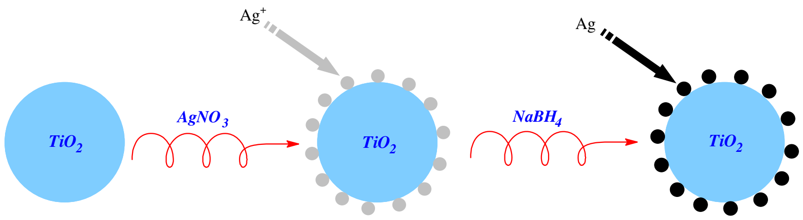

Fig. 1. Scheme of the preparation of Ag/$TiO_2$ nanoparticles.

room temperature with pH of about 6.5, which is the natural pH of the reaction medium.

The photocatalytic degradation of CAP and TAZ follows a pseudo-first-order kinetics which is generally expected from an Ag/$TiO_2$ photocatalytic degradation system. The pseudo-first-order rate constant, $k_{app}$ was determined from the slope of $\ln(C/C_0)$ vs irradiation time according to the following relation:

$$-\ln\frac{C}{C_0} = k_{app}t \tag{1}$$

where $t$ is the irradiation time, $C_0$ is the initial concentration of pollutant (mg/L), and $C$ is the concentration of pollutant (mg/L) at time $t$ [28].

### 2.4. Characterization and analytical methods

The crystalline phase of nanoparticles were analyzed by XRD measurements by using Siemens XRD-D5000 ($\lambda = 0.154$ nm). Morphological studies were conducted using a SEM (SEM, Viga II, $3 \times 10^5$, USA) equipped with a probe for the energy dispersive X-ray microanalysis (EDX). The surface properties were observed under TEM (PHILIPS CM 10–100 keV). The surface chemical composition of samples was analyzed by XPS (XPS, twin anode XR3E2 X-ray source). All the binding energies were referenced to the C1s peak at 284.8 eV of surface adventitious carbon. An ultrasonic bath from Elma (model T 460/H, Singen, Germany) was used for the sonication of samples. A UV lamp (15 W, UV-C, $\lambda_{max} = 254$ nm, manufactured by Philips, Holland) was used as the excitation source. Additionally, a UV–vis spectrophotometer (Ultrospec 2000, England) was used for the measurement of the concentration of CAP and TAZ. Finally, concentration of TOC in the solution was measured using a TOC analyzer (Shimadzu, TOC-$V_{CSH}$).

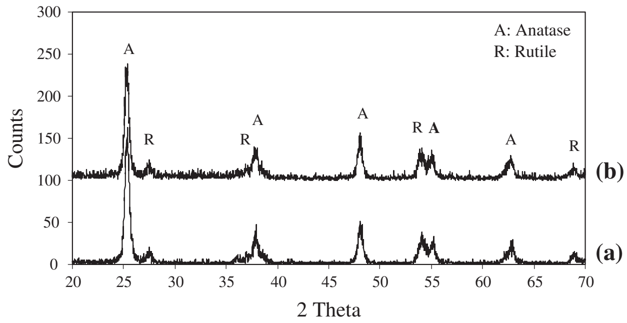

Fig. 2. XRD patterns of: (a) pure $TiO_2$ and (b) 1.5 wt.% Ag/$TiO_2$ nanoparticles.

## 3. Results and discussion

### 3.1. The characterization of silver doped $TiO_2$ nanoparticles

Fig. 2(a) and (b) shows the XRD pattern of pure and silver-modified $TiO_2$ powders by the optimum amounts of Ag prepared by chemical reduction method. The peaks in the XRD patterns correspond to the anatase and rutile phases of the pure $TiO_2$. The results reveal that there is no difference between the XRD patterns of the prepared nanoparticles and that of the pure $TiO_2$. No sign of Ag crystals is seen in the XRD results obtained from both calcined and noncalcined samples at all Ag-loaded concentrations suggesting that either the Ag is not in the crystal form or the extent of deposition is not detectable by XRD analysis. This may also be due to the fact that loading does not alter the crystal structure of Ag/$TiO_2$ [18].

Both the photocatalysts $TiO_2$ and silver-modified $TiO_2$ were characterized by the SEM to determine the morphology of $TiO_2$ and Ag/$TiO_2$ nanoparticles. Comparison of the SEM micrographs of pure $TiO_2$ and Ag/$TiO_2$ nanoparticles proved that loading of Ag nanoparticles did not affect the spherical shape of $TiO_2$ particles (Fig. 3). The EDX analysis (Fig. 4) also confirmed the loading of Ag on $TiO_2$.

The TEM image of the Ag/$TiO_2$ nanoparticles prepared by chemical reduction is shown in Fig. 5. The shape and size of the titanium crystallites were unchanged as a result of surface modification by silver particles. The silver particles (black dots indicated) were located on the surface of the individual $TiO_2$ nanoparticles. Also, there is a possibility for silver to be incorporated into the interstitial positions of the semiconductor particles [29]. The estimated range of the deposited silver nanoparticles was 2–10 nm. Agglomerates of metallic silver were also observed on $TiO_2$ in addition to small Ag particles.

To confirm the metallic state of the silver on the surface of these samples, the resultant catalyst samples were further characterized by XPS measurement. Fig. 6(a) and (b) shows the XPS profiles of the prepared Ag/$TiO_2$ nanoparticles. Besides, sharp peaks for Ti, O, Ag, and C are detected. Fig. 6(b) is Ag 3d core level XPS scan over smaller energy windows at higher resolution. The Ag 3d5/2 peak appeared at a binding energy of 367.3 eV and the splitting of the 3d doublet is 6.0 eV. This binding energy indicates that Ag mainly exists in the $Ag^0$ state on the $TiO_2$ nanoparticle surface [30,31].

### 3.2. Photocatalytic activity studies

According to Fig. 7, the photocatalytic degradation rates of the pollutants under similar conditions,

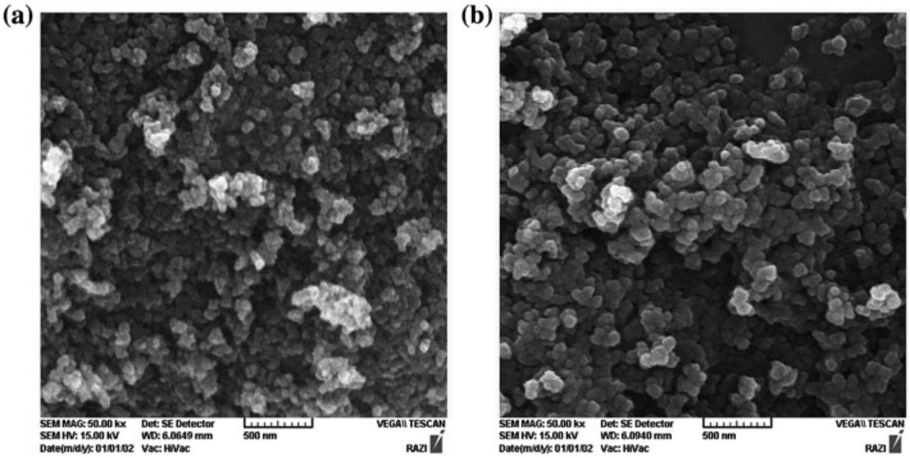

Fig. 3. SEM micrograph of: (a) pure $TiO_2$ and (b) 1.5 wt.% $Ag/TiO_2$ nanoparticles.

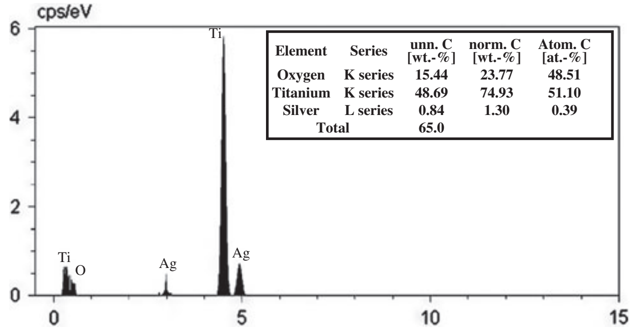

| Element | Series | unn. C [wt.-%] | norm. C [wt.-%] | Atom. C [at.-%] |
|---|---|---|---|---|
| Oxygen | K series | 15.44 | 23.77 | 48.51 |
| Titanium | K series | 48.69 | 74.93 | 51.10 |
| Silver | L series | 0.84 | 1.30 | 0.39 |
| Total | | 65.0 | | |

Fig. 4. EDX analysis of 1.5 wt.% $Ag/TiO_2$ nanoparticles.

notably, depend on the activity of the used catalyst. Results showed that the $Ag/TiO_2$ catalyst is more active than pure $TiO_2$ at degradation of CAP and TAZ. It was also observed from this Figure. that TAZ can undergo fast photocatalytic degradation compared with CAP. Based on the comparative studies, it may be inferred that the effect of silver metal depends strongly on the kind of pollutants. As mentioned in the introduction part, the electron and the hole are generated upon irradiation of a semiconductor surface. A semiconductor is characterized by an electronic band structure in which the highest occupied energy band of a semiconductor called valence bond (vb), and the lowest empty band called conduction band (cb) are separated by a band gap. Heterogeneous photocatalysis is a process in which a photon of energy higher or equal to the band gap energy is absorbed by a semiconductor particle like $TiO_2$ promoting an electron from the vb to the cb with simultaneous generation of a hole ($h^+$) in the vb.

As it can be observed from Fig. 8, when $TiO_2$ is illuminated with the light, an electron excites out of its energy level and consequently leaves a hole in the vb. Indeed, electrons are promoted from the vb to the cb of $TiO_2$ to give electron–hole pairs Eq. (2). The holes at the $TiO_2$ vb can oxidize the adsorbed water or hydroxide ions to produce hydroxyl radicals Eqs. (3) and (4).

$$TiO_2 + hv \rightarrow e^-_{cb} + h^+_{vb} \tag{2}$$

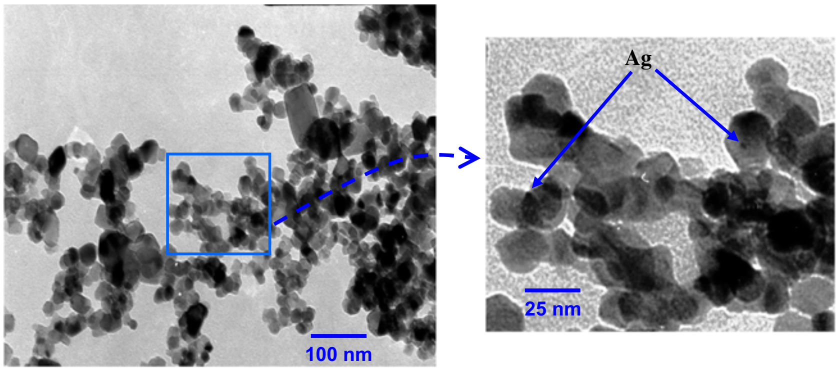

Fig. 5. TEM micrograph of 1.5 wt.% $Ag/TiO_2$ nanoparticles.

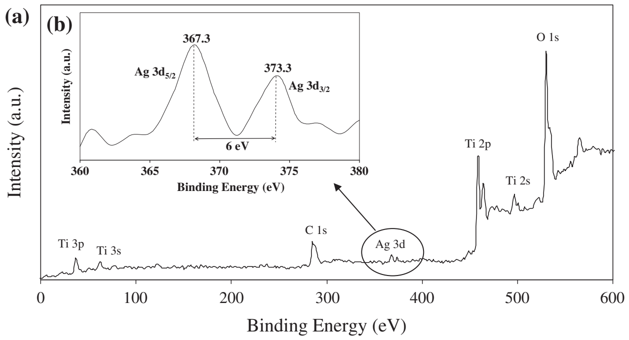

Fig. 6. XPS spectra of (a) Ag/$TiO_2$ nanoparticles and (b) The high resolution spectrum of Ag 3d region.

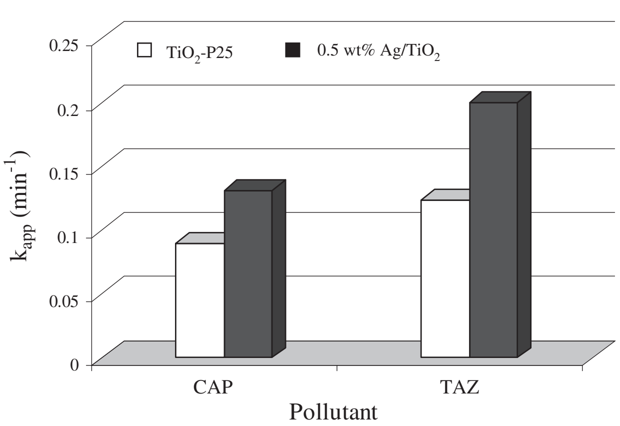

Fig. 7. Pseudo-first-order kinetics of the photocatalytic degradation of the CAP and TAZ. $I_o = 50\,W/m^2$, $[Pollutant]_o = 20\,mg/L$, $[Catalyst] = 400\,mg/L$.

$$h_{vb}^{+} + H_2O_{ads} \rightarrow {}^{\cdot}OH + H^{+} \quad (3)$$

$$h_{vb}^{+} + OH_{ads} \rightarrow {}^{\cdot}OH \quad (4)$$

Electron in the cb on the catalyst surface can reduce molecular oxygen to superoxide radical anion Eq. (5). This radical may form hydrogen peroxide Eq. (6).

$$e_{cb}^{-} + O_2 \rightarrow {}^{\cdot}O_2^{-} \quad (5)$$

$${}^{\cdot}O_2^{-} + HO_2^{\cdot} + H^{+} \rightarrow H_2O_2 + O_2 \quad (6)$$

The hydroxyl radical is a powerful oxidizing agent and attacks the organic matter (OM), and intermediates (Int.) are formed. These intermediates react with hydroxyl radicals to produce final products (*P*) Eq. (7) [7,28].

$${}^{\cdot}OH_{ads} + OM \rightarrow Int. \rightarrow P \quad (7)$$

The phenomenon of electron–hole recombination is extremely efficient in the absence of a proper acceptor or donor and hence represents the major energy-wasting step. In bare or pure $TiO_2$, about 90% of the excited charge carriers (electron and hole) get recombined rapidly within and/or at the surface of $TiO_2$ particles and hence a poor photocatalytic performance is observed. Silver and other noble metal are very effective traps for the excited electrons. The enhancing effect of silver at degradation of CAP and TAZ may be explained by its ability to trap electrons. They act as electron scavengers. This process reduces

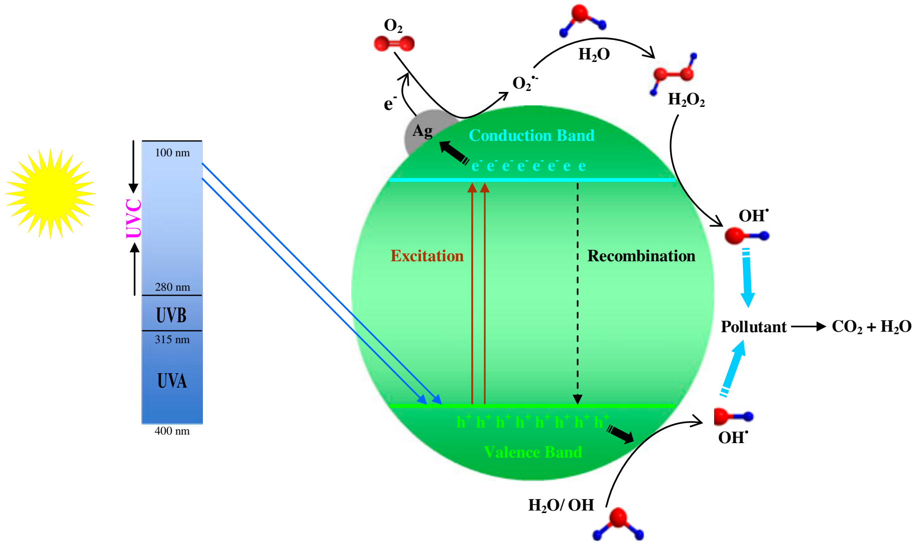

Fig. 8. Mechanism of the photocatalytic action of Ag/$TiO_2$ nanoparticles under UV light irradiation.

the recombination of charges and favors oxidation of substrate by producing more $^{\bullet}OH$. Accordingly, loading Ag metals onto the $TiO_2$ surface can expedite the transport of photo-excited electrons to the outer systems [18,32]. The adsorbed oxygen on the photocatalyst surface traps the electrons and produces superoxide anion. On the other hand, holes on the $TiO_2$ surface can oxidize adsorbed water or hydroxide ions to produce hydroxyl radicals [33].

### 3.3. The effect of silver concentration

The resulting $k_{app}$ values provided in Fig. 9 show that the degradation of CAP and TAZ increases significantly when rising Ag loading on $TiO_2$ surface from 0.0 to 1.5 wt.% reaches a maximum at 1.5 wt.%, and then decreases with the further increasing of Ag loading. Consequently, it can be inferred that the optimum Ag loading is 1.5 wt.%, which is consistent with the result of photocurrent.

The effect of silver on the degradation of organic pollutants is not consistent and varies from study to study. Shokri et al. and Subba Rao et al., for instance, observed beneficial effect of the presence of silver for the degradation of CAP and TAZ, respectively [19,27]. Lam et al., however, found that photocatalytic decomposition of resorcinol was slightly enhanced in the presence of $Ag/TiO_2$ [34]. Based on the comparative studies, it may be inferred that the effect of silver depends strongly on the kind of pollutants, however, is always favorable for the degradation of pollutants.

Silver nanoparticles deposited on the titanium dioxide surface can act as electron–hole separation centers resulting in the formation of Shottky barrier at the metal–semiconductor contact region, which improves the charge separation and thus enhances the photocatalytic activity of $TiO_2$. In contrast, when the silver amount is above its optimum, the silver nanoparticles can also act as recombination centers which results in decreasing the photocatalytic activity of $TiO_2$ [35]. The detrimental effect of silver on $TiO_2$ has several reasons:

- The probability for the hole capture is increased by the large number of negatively-charged silver particles on $TiO_2$ at high silver content, which reduces the efficiency of charge separation [3,32].
- Excessive coverage of $TiO_2$ catalyst with Ag nanoparticles limits the amount of light reaching to the $TiO_2$ surface, reducing the number of photogenerated $e^- - h^+$ pairs and consequently lowering the $TiO_2$ photoactivity [36].

By comparing the pseudo-first-order rate constant for pure $TiO_2$ with $Ag/TiO_2$ prepared by chemical reduction method (Fig. 9), it can be clearly observed that the photodegradation rate of TAZ at all percentages of Ag-loading is significantly higher than that of CAP.

### 3.4. The effect of photocatalyst concentration

Compared with pure $TiO_2$, $TiO_2$ modified with 1.5 wt.% (optimum value) of Ag at photodegradation of CAP and TAZ, at different amounts of catalyst from 0.0 to 1,200 mg/L shows that the rate constant increases with increasing the amount of $Ag/TiO_2$ catalyst until 800 mg/L for TAZ and 1,000 mg/L for CAP (Fig. 10). An increment in the amount of catalyst increased the number of active sites on the catalyst surface and that in turn increased the number of hydroxyl radicals [1]. When the concentration of $Ag/TiO_2$ catalyst was increased above the limiting value, the degradation rate decreased due to an increase in the turbidity of the suspension and a decrease in UV light penetration as a result of increased scattering effect [37,38]. The obtained results indicated that the photodegradation rate in the presence of all catalysts,

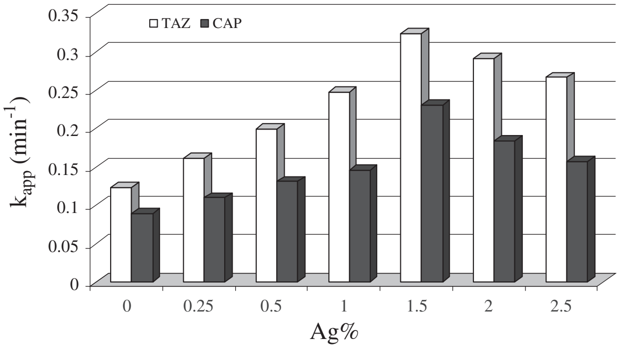

Fig. 9. Effect of silver concentration on the photoactivity of $TiO_2$ nanoparticles at degradation of CAP and TAZ. $I_o = 50\,W/m^2$, $[Pollutant]_o = 20\,mg/L$, $[Catalyst] = 400\,mg/L$.

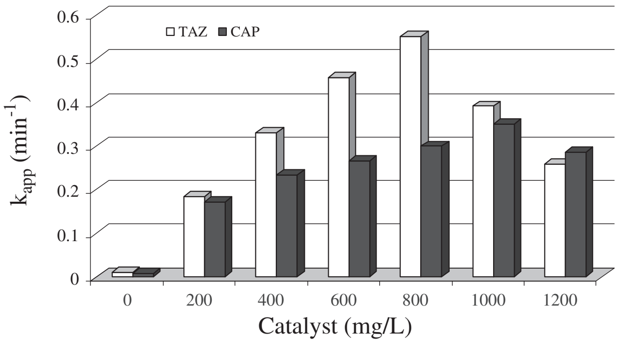

Fig. 10. Effect of photocatalyst loading of pure and $Ag/TiO_2$ nanoparticles at degradation of CAP and TAZ. $I_o = 50\,W/m^2$, $[Pollutant]_o = 20\,mg/L$.

except at amounts of catalyst of 1,200 mg/L, is slowed down with CAP solution in comparison with TAZ solution.

Many other examples could be presented here demonstrating the different optimum catalyst loading for the different investigations. Gupta et al. [23], for instance, found that the optimum catalyst loading for the best degradation of TAZ is 0.18 mg/L. In another study, on the other hand, the optimum catalyst concentration was found to be 900 mg/L [19]. This limit depends on the geometry and working conditions of the photoreactor, concentration, and nature of organic molecules and a defined amount of catalyst in which all the particles, i.e. the entire surface exposed, are totally illuminated.

### 3.5. The effect of initial CAP and TAZ concentration

The initial concentration of CAP and TAZ in a given catalytic reaction is also another factor which needs to be taken into account. The effect of this factor on the degree of photodegradation was studied by varying the initial concentration over a range of 10–30 mg/L at the optimum conditions. In the presence of Ag/$TiO_2$ catalyst, the photodegradation rate of CAP and TAZ was shown to decrease with the increase in initial concentration (Fig. 11). At high CAP and TAZ concentration, the adsorbed reactant molecules may occupy all the active sites of catalyst surface, and this leads to decrease in degradation rate. Furthermore, as the concentration of target pollutant increases, more and more molecules of the compound get adsorbed on the surface of the catalyst. Therefore, the requirement of reactive species ($^{\cdot}OH$) needed for the degradation of pollutant also increases. Once the concentration of the target pollutant is increased, it also causes the pollutant molecules to absorb light, and photons never reach the catalyst surface and thus, the photodegradation rate decreases [1,36,39,40].

### 3.6. The effect of light intensity

Light intensity is also an important parameter that influenced the decomposition of pollutants by photocatalytic processes. Fig. 12 depicts the effect of light intensity on the photodegradation rate of CAP and TAZ. The increase of radiation intensity from 10 to 50 $W/m^2$ increases the pseudo-first-order rate constant. This phenomenon implies that the UV irradiation generates the photons required for the electron transfer from the vb to the cb of the catalyst, and the energy of a photon is related to its wavelength and the overall energy input to a photocatalytic process is dependent on light intensity. The rate of degradation increases when more radiations fall on the catalyst surface and hence more hydroxyl radicals are produced [41–43].

### 3.7. The effect of calcination temperature

In order to study the influence of the calcination temperature on the photocatalytic activity of the catalyst, the 1.5 wt.% Ag/$TiO_2$ was calcined at 300, 500, and 700°C for 3 h while other experimental conditions were kept constant. Results in Fig. 13 reveal that the photocatalytic activity of Ag/$TiO_2$ nanoparticles decreases with increase in calcination temperature from 300 to 700°C. This reduction in activities of nanoparticles can be justified due to the increase in crystallite size of nanoparticles, agglomeration of nanoparticles, and transformation of anatase to rutile phase [44–46].

### 3.8. Photocatalytic mineralization of CAP and TAZ

Mineralization of CAP and TAZ in photocatalytic degradation process using $TiO_2$ modified with varying

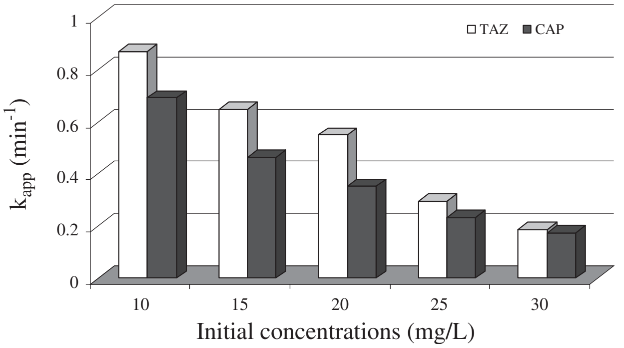

Fig. 11. Effect of initial concentration on photocatalytic degradation of CAP and TAZ. $I_o$ = 50 $W/m^2$, 1.5 wt.% Ag/$TiO_2$ nanoparticles, $[Catalyst]_{CAP}$ = 1,000 mg/L, $[Catalyst]_{TAZ}$ = 800 mg/L.

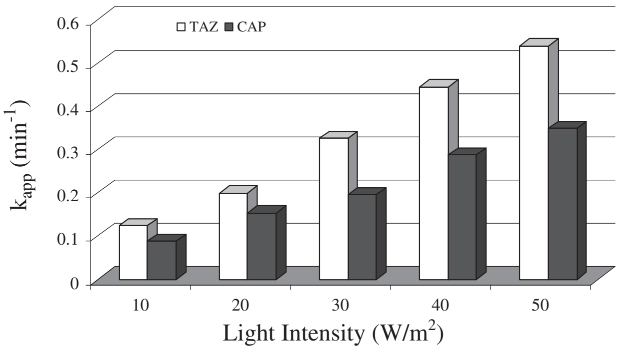

Fig. 12. Effect of UV light intensity on the degradation rate constant of CAP and TAZ. $[Pollutant]_o$ = 20 mg/L, 1.5 wt.% Ag/$TiO_2$ nanoparticles, $[Catalyst]_{CAP}$ = 1,000 mg/L, $[Catalyst]_{TAZ}$ = 800 mg/L.

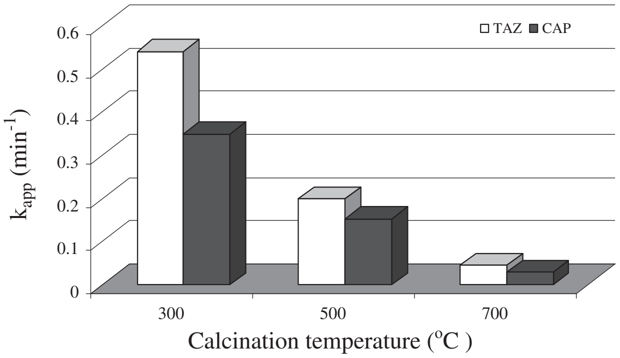

Fig. 13. Effect of calcination temperature on photocatalytic activity of Ag/$TiO_2$ nanparticles. $[Pollutant]_o = 20$ mg/L, 1.5 wt.% Ag/$TiO_2$ nanoparticles, $[Catalyst]_{CAP} = 1{,}000$ mg/L, $[Catalyst]_{TAZ} = 800$ mg/L.

Table 2
Reduction in the TOC value (%) of CAP and TAZ solution using Ag/$TiO_2$ catalysts with different Ag loading. $I_o$ = 50 W/m$^2$, [CAP & TAZ]$_o$ = 20 mg/L, [Catalyst] = 400 mg/L, irradiation time = 120 min

| Catalyst | Reduction in the TOC value (%) | |
|---|---|---|
| | CAP | TAZ |
| 0.25 wt.% Ag/$TiO_2$ | 49 | 58 |
| 0.50 wt.% Ag/$TiO_2$ | 55 | 67 |
| 1.00 wt.% Ag/$TiO_2$ | 63 | 70 |
| 1.50 wt.% Ag/$TiO_2$ | 84 | 89 |
| 2.00 wt.% Ag/$TiO_2$ | 47 | 53 |
| 2.50 wt.% Ag/$TiO_2$ | 41 | 48 |

amounts of silver for 120 min is studied with 20 mg/L of each pollutant solutions. In order to assess the degree of mineralization obtained during the photocatalytic treatment, the formation of $CO_2$ and inorganic ions is generally determined. The term "photocatalytic degradation" usually refers to complete photocatalytic oxidation or photomineralization, essentially to $CO_2$, $H_2O$, $NO_3^-$, $PO_4^{3-}$, and halide ions [28]. By comparing the TOC values for $TiO_2$ modified with varying amounts of silver (Table 2), it can be clearly observed that the reduction in the TOC value in the presence of 1.5 wt.% Ag/$TiO_2$ is significantly higher when the other catalyst was used. The obtained results also indicated that reduction in the TOC value in the presence of all catalysts is lesser than with CAP solution in comparison with TAZ solution.

## 4. Conclusion

Photocatalytic degradation of CAP and TAZ was studied in the aqueous suspensions of silver-modified $TiO_2$ (Ag/$TiO_2$) nanoparticles under ultraviolet (UV) light irradiation. Ag/$TiO_2$ nanoparticles were prepared with chemical reduction method and characterized by XRD, SEM, EDX, TEM, and XPS techniques. XPS measurement indicates that Ag mainly exists in the $Ag^0$ state on the $TiO_2$ nanoparticles surface. The study included the investigation of the effect of various parameters, such as silver concentration, photocatalyst loading, initial substrate concentration, light intensity, and calcination temperature. The main conclusions drawn from this study are summarized as follows:

- Treatment efficiency depends on the operating conditions employed, such as silver concentration, photocatalyst loading, initial substrate concentration, light intensity, and calcination temperature.
- TAZ is generally more susceptible to photocatalytic degradation than CAP. Differences in reactivity are likely to be due to the different chemical structures.
- Reduction in the TOC value in the presence of all catalysts is lesser than with CAP solution in comparison with TAZ solution.

## Acknowledgment

The author would like to thank the financial support of the Islamic Azad University-Shahindezh branch and the Iranian Nanotechnology Initiative Council.

## Symbols

| | | |
|---|---|---|
| $C_0$ | — | initial concentration of pollutant, mg/L |
| $C$ | — | concentration of pollutant (mg/L) at time $t$ |
| $t$ | — | irradiation time |
| $k_{app}$ | — | pseudo-first-order rate constant |

## References

[1] M.A. Behnajady, N. Modirshahla, R. Hamzavi, Kinetic study on photocatalytic degradation of C.I. acid yellow 23 by ZnO photocatalyst, J. Hazard. Mater. B 133 (2006) 226–232.
[2] S. Pura, G. Atun, Adsorptive removal of acid blue 113 and tartrazine by fly ash from single and binary dye solutions, Sep. Sci. Technol. 44 (2009) 75–101.
[3] N. Sobana, K. Selvam, M. Swaminathan, Optimization of photocatalytic degradation conditions of direct red 23 using nano-Ag doped $TiO_2$, Sep. Purif. Technol. 62 (2008) 648–653.
[4] N.K. Daud, U.G. Akpan, B.H. Hameed, Decolorization of sunzol black DN conc. in aqueous solution by Fenton oxidation process: Effect of system parameters and kinetic study, Desalin. Water Treat. 37 (2012) 1–7.
[5] T. Herberer, Occurrence, fate, and removal of pharmaceutical residues in the aquatic environment: A review of recent research data, Toxicol. Lett. 131 (2002) 5–17.
[6] B. Halling-Sørensen, S. Nors Nielsen, P.F. Lanzky, F. Ingerslev, H.C. Holten Lützhøft, S.E. Jørgensen, Occurrence, fate and effects of pharmaceutical substances in the environment – a review, Chemosphere 36 (1998) 357–393.

[7] E.S. Elmolla, M. Chaudhuri, Photocatalytic degradation of amoxicillin, ampicillin and cloxacillin antibiotics in aqueous solution using UV/$TiO_2$ and UV/$H_2O_2$/$TiO_2$ photocatalysis, Desalination 252 (2010) 46–52.

[8] M. El-Kemary, H. El-Shamy, I. El-Mehasseb, Photocatalytic degradation of ciprofloxacin drug in water using ZnO nanoparticles, J. Lumin. 130 (2010) 2327–2331.

[9] A. Chatzitakis, C. Berberdou, I. Paspaltsis, G. Kyriakou, T. Sklaviadis, I. Poulios, Photocatalytic degradation and drug activity reduction of chloramphenicol, Water Res. 42 (2008) 386–394.

[10] J. Zhang, D. Fu, Y. Xu, C. Liu, Optimization of parameters on photocatalytic degradation of chloramphenicol using $TiO_2$ as photocatalyist by response surface methodology, J. Environ. Sci. 22 (2010) 1281–1289.

[11] E. Hapeshi, A. Achilleos, M.I. Vasquez, C. Michael, N.P. Xekoukoulotakis, D. Mantzavinos, D. Kassinos, Drugs degrading photocatalytically: Kinetics and mechanisms of ofloxacin and atenolol removal on titania suspensions, Water Res. 44 (2010) 1737–1746.

[12] E.S. Elmolla, M. Chaudhuri, Comparison of different advanced oxidation processes for treatment of antibiotic, Desalination 256 (2010) 43–47.

[13] M. Petala, V. Tsiridis, P. Samaras, A. Zouboulis, G.P. Sakellaropoulos, Wastewater reclamation by advanced treatment of secondary effluents, Desalination 195 (2006) 109–118.

[14] C. Chen, X. Zhang, W. He, W. Lu, H. Han, Comparison of seven kinds of drinking water treatment processes to enhance organic material removal: A pilot test, Sci. Total Environ. 382 (2007) 93–102.

[15] A. Fujishima, X. Zhang, D.A. Tryk, $TiO_2$ photocatalysis and related surface phenomena, Surf. Sci. Rep. 63 (2008) 515–582.

[16] S. Sakthivel, M.V. Shankar, M. Palanichamy, B. Arabindoo, D.W. Bahnemann, V. Murugesan, Enhancement of photocatalytic activity by metal deposition: characterisation and photonic efficiency of Pt, Au and Pd deposited on $TiO_2$ catalyst, Water Res. 38 (2004) 3001–3008.

[17] M. Kotobuki, R. Leppelt, D.A. Hansgen, D. Widmann, R.J. Behm, Reactive oxygen on a Au/$TiO_2$ supported catalyst, J. Catal. 264 (2009) 67–76.

[18] M.A. Behnajady, N. Modirshahla, M. Shokri, B. Rad, Enhancement of photocatalytic activity of $TiO_2$ nanoparticles by silver doping: photodeposition versus liquid impregnation methods, Global Nest J. 10 (2008) 1–7.

[19] M. Shokri, A. Jodat, N. Modirshahla, M.A. Behnajady, Photocatalytic degradation of chloramphenicol in an aqueous suspension of silver-doped $TiO_2$ nanoparticles, Environ. Technol. iFirst (2012) 1–6.

[20] R. Nainani, P. Thakur, M. Chaskar, Synthesis of silver doped $TiO_2$ nanoparticles for the improved photocatalytic degradation of methyl orange, J. Mater. Sci. Eng. B 2 (2012) 52–58.

[21] A.A. Abdel-Wahab, O.S. Mohamed, S.A. Ahmed, M.F. Mostafa, Ag-doped $TiO_2$ enhanced photocatalytic oxidation of 1,2-cyclohexanediol, J. Phys. Org. Chem. 25 (2012) 1418–1421.

[22] N. Nino-Martinez, G.A. Martinez-Castanon, A. Aragon-Pina, F. Martinez-utierrez, J.R. Martinez-Mendoza, F. Ruiz, Characterization of silver nanoparticles synthesized on titanium dioxide fine particles, Nanotechnology 19 (2008) 065711/1–065711/8.

[23] V.K. Gupta, R. Jain, A. Nayak, S. Agarwal, M. Shrivastava, Removal of the hazardous dye—tartrazine by photodegradation on titanium dioxide surface, Mater. Sci. Eng. C (2011) 1062–1067.

[24] M.G. Dias, E.B. Azevedo, Photocatalytic decolorization of commercial acid dyes using solar irradiation, Water Air Soil Pollut. 204 (2009) 79–87.

[25] A.K. Gupta, A. Pal, C. Sahoo, Photocatalytic degradation of a mixture of crystal violet (basic violet 3) and methyl red dye in aqueous suspensions using AgC doped $TiO_2$, Dyes Pigments 69 (2006) 224–232.

[26] A.R. Khataee, M.N. Pons, O. Zahraa, Photocatalytic degradation of three azo dyes using immobilized $TiO_2$ nanoparticles on glass plates activated by UV light irradiation: Influence of dye molecular structure, J. Hazard. Mater. 168 (2009) 451–457.

[27] K.V. Subba Rao, B. Lavédrine, P. Boule, Influence of metallic species on $TiO_2$ for the photocatalytic degradation of dyes and dye intermediates, J. Photochem. Photobiol. A 154 (2003) 189–193.

[28] I.K. Konstantinou, T.A. Albanis, $TiO_2$-assisted photocatalytic degradation of azo dyes in aqueous solution: kinetic and mechanistic investigations, Appl. Catal. B 49 (2004) 1–14.

[29] S. Anandan, P. Sathish Kumar, N. Pugazhenthiran, J. Madhavan, P. Maruthamuthu, Effect of loaded silver nanoparticles on $TiO_2$ for photocatalytic degradation of acid red 88, Sol. Energy Mater. Sol. Cells 92 (2008) 929–937.

[30] L. Sun, J. Li, C. Wang, S. Li, Y. Lai, H. Chen, C. Lin, Ultrasound aided photochemical synthesis of Ag loaded $TiO_2$ nanotube arrays to enhance photocatalytic activity, J. Hazard. Mater. 171 (2009) 1045–1050.

[31] J. Yu, J. Xiong, B. Cheng, S. Liu, Fabrication and characterization of Ag–$TiO_2$ multiphase nanocomposite thin films with enhanced photocatalytic activity, Appl. Catal. B-Environ. 60 (2005) 211–221.

[32] M.A. Behnajady, N. Modirshahla, M. Shokri, A. Zeininezhad, H.A. Zamani, Enhancement photocatalytic activity of ZnO nanoparticles by silver doping with optimization of photodeposition method parameters, J. Environ. Sci. Health, Part A 44 (2009) 666–672.

[33] N. Daneshvar, M. Rabbani, N. Modirshahla, M.A. Behnajady, Kinetic modeling of photocatalytic degradation of acid red 27 in UV/$TiO_2$ process, J. Photochem. Photobiol. A, 168 (2004) 39–45.

[34] S.W. Lam, K. Chiang, T.M. Lim, R. Amal, G.K.-C. Low, The effect of platinum and silver deposits in the photocatalytic oxidation of resorcinol, Appl. Catal. B 72 (2007) 363–372.

[35] A. Zielinska, E. Kowalska, J.W. Sobczak, I. Łacka, M. Gazda, B. Ohtani, J. Hupka, A. Zaleska, Silver-doped $TiO_2$ prepared by microemulsion method: Surface properties, bio- and photoactivity, Sep. Purif. Technol. 72 (2010) 309–318.

[36] O. Carp, C.L. Huisman, A. Reller, Photoinduced reactivity of titanium dioxide, Prog. Solid State Chem. 32 (2004) 33–177.

[37] M.A. Behnajady, N. Modirshahla, N. Daneshvar, M. Rabbani, Photocatalytic degradation of an azo dye in a tubular continuous-flow photoreactor with immobilized $TiO_2$ on glass plates, Chem. Eng. J. 127 (2007) 167–176.

[38] N. Daneshvar, D. Salari, A.R. Khataee, Photocatalytic degradation of azo dye acid red 14 in water on ZnO as an alternative catalyst to $TiO_2$, J. Photochem. Photobiol. A 162 (2004) 317–322.

[39] N. Modirshahla, A. Hassani, M.A. Behnajady, R. Rahbarfam, Effect of operational parameters on decolorization of Acid Yellow 23 from wastewater by UV irradiation using ZnO and ZnO/$SnO_2$ photocatalysts, Desalination 271 (2011) 187–192.

[40] N. Daneshvar, M. Rabbani, N. Modirshahla, M.A. Behnajady, Kinetic modeling of photocatalytic degradation of acid red 27 in UV/$TiO_2$ process, J. Photochem. Photobiol. A 168 (2004) 39–45.

[41] P. Chin, L.P. Yang, D.F. Ollis, Formaldehyde removal from air via a rotating adsorbent combined with a photocatalyst reactor: Kinetic modelling, J. Catal. 237 (2006) 29–37.

[42] A.A. Khodja, T. Sehili, J. Pilichowski, P. Boulez, Photocatalytic degradation of 2 phenyl-phenols on $TiO_2$ and ZnO in aqueous suspension, J. Photochem. Photobiol. A 141 (2001) 231–239.

[43] R. Pourata, A.R. Khataee, S. Aber, N. Daneshvar, Removal of the herbicide Bentazon from contaminated water in the presence of synthesized nanocrystalline $TiO_2$ powders under irradiation of UV-C light, Desalination 249 (2009) 301–307.

[44] S. Watson, D. Beydoun, J. Scott, R. Amal, Preparation of nanosized crystalline $TiO_2$ particles at low temperature for photocatalysis, J. Nanopart. Res. 6 (2004) 193–207.

[45] H.-I. Hsiang, S.-C. Lin, Effects of aging on nanocrystalline anatase-to-rutile phase transformation kinetics, Ceram. Int. 34 (2008) 557–561.

[46] U.G. Akpan, B.H. Hameed, Parameters affecting the photocatalytic degradation of dyes using $TiO_2$-based photocatalysts: A review, J. Hazard. Mater. 170 (2009) 520–529.